Journal of Biomedical Optics

BiomedicalOptics.SPIEDigitalLibrary.org

Gaussian beam in two-photon fluorescence imaging of rat brain microvessel

Lingyan Shi
Adrián Rodríguez-Contreras
Robert R. Alfano

SPIE.

Journal of Biomedical Optics 19(12), 126006 (December 2014)

TECHNICAL NOTE

Gaussian beam in two-photon fluorescence imaging of rat brain microvessel

Lingyan Shi,[a,b,c,*] Adrián Rodríguez-Contreras,[b,c] and Robert R. Alfano[c]
[a]The City College of New York, Department of Biomedical Engineering, 160 Convent Avenue, New York, New York 10031, United States
[b]The City College of New York, Department of Biology, 160 Convent Avenue, New York, New York 10031, United States
[c]The City College of New York, Institute for Ultrafast Spectroscopy and Lasers and Departments of Electrical Engineering and Physics, 160 Convent Avenue, New York, New York 10031, United States

Abstract. The critical optical properties of a Gaussian laser beam in two-photon or multiphoton fluorescence imaging, including the beam spot size, depth of focus, and intensity profile, are investigated for spatially locating nanoscale solutes in and surrounding the microvessels of rat brain. [DOI: 10.1117/1.JBO.19.12.126006]

Keywords: Gaussian beam; two-photon microscopy; spot size; depth of focus; rat brain; *in vivo*.

Paper 140614TNR received Sep. 25, 2014; accepted for publication Nov. 5, 2014; published online Dec. 9, 2014.

1 Introduction

A Gaussian (G) beam is an ideal spatial form of a laser beam and one of a larger class of Laguerre–Gaussian solutions (LG) of the wave equation with orbital angular momentum L. The G beam at $L = 0$ is the fundamental transverse mode (TEM_{00}) of the laser and is used to focus into material with a lens which takes a Fourier transform (FT). It is used in optical physics for propagating electro-magnetic energy in space with light-matter interactions. The profile of the G beam is a key element for imaging in multiphoton microscopy, including two-photon (2P) and three-photon (3P) applications, where a 140-fs pulsed G beam is used in the near-infrared to image objects in two-dimensional (2-D) and three-dimensional (3-D), particularly for cellular structures in the brain and other biological systems.

There are several salient properties of G beam in the nonlinear optical process of two-photon fluorescence (2PF) as the beam propagates and scans in the x, y, z directions: beam spot size, depth of focus (DOF), intensity profile in radial (r, x, y) directions, and propagation in z direction. The propagation for G beam in media has been reviewed by Saleh and Teich [1] and Yariv,[2] but other features for small-scale emitters, such as dyes or quantum dots (QDs) in microscale biological tissues or media, have not been examined. This technical note investigates the important optical parameters and features of G beam in 2P microscopy for small nanometer-scale emitters in media, and examines the influence of these parameters on imaging microvessels in rat brain *in vivo*.

2 Materials and Methods

2.1 *Gaussian Beam Model*

The intensity profile I_G of a G beam is given by

$$I_G(r,z) = I_0\left[\frac{w_0}{w(z)}\right]^2 \exp\left[-\frac{2r^2}{w^2(z)}\right], \quad (1)$$

where I_0 is the incident intensity, r is the transverse radius, z is the path length, w_0 is the narrowest spot size (also known as beam waist), which equals $1/e$ of Gaussian electric field (E_G), and $w(z)$ is the spot size given by[1,2]

$$w^2(z) = w_0^2\left[1 + \left(\frac{z}{z_0}\right)^2\right], \quad (2)$$

$$z_0 = \frac{\pi w_0^2}{\lambda}, \quad (3)$$

where z_0 is the Rayleigh length (Fig. 1) and λ is the wavelength. Length $2z_0$ is the DOF. At the beam waist ($r = w_0$, $z = 0$, Fig. 1), the Gaussian beam electric field drops to $1/e$ of E_0 (the maximum electric field) and the intensity drops to $1/e^2$ of I_0. From Eq. (1), the intensity along z axis ($r = 0$) is

$$I_G(0,z) = I_0\frac{1}{1 + (z/z_0)^2}, \quad (4)$$

which is an oval spanning $2z_0$ and with the maximum intensity at $z = 0$. The intensity reduces to $1/2I_0$ at z_0 [Fig. 2(a)]. The DOF is the critical distance for G beam intensity in the z direction, which depends on the magnification (40×, 20×, etc.) and numerical aperture (NA) of the microscope objective lens used. The NA is given by

$$\mathrm{NA} = n\frac{D}{2f}, \quad (5)$$

where n is the index of refraction, D is the diameter of the lens, and f is the focal length. The DOF ($2z_0$) is given by

$$2z_0 = \frac{2\pi w_0^2}{\lambda}, \quad (6)$$

where

*Address all correspondence to: Lingyan Shi, E-mail: lshi00@citymail.cuny.edu

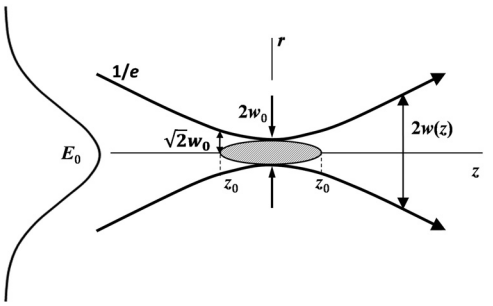

Fig. 1 Illustration of the key spatial electric field profile of a Gaussian beam. E_0, the maximum incident electric field at the origin; r, the transverse radius; z, path length; z_0, the Rayleigh length; $w(z)$, spot size; w_0, the narrowest spot size (beam waist). The electric field amplitude of Gaussian beam is given by $|E_G(r,z)| = E_0[w_0/w(z)]\exp[(-r^2)/w(z)^2]$.

$$w_0 = \frac{\lambda}{\pi \mathrm{NA}}. \tag{7}$$

Thus, the relationship between the DOF and NA of the objective lens is

$$2z_0 = \frac{2\lambda}{\pi \mathrm{NA}^2}. \tag{8}$$

The beam waist (w_0) and DOF ($2z_0$) are two of the most salient features used to locate dyes or QDs in tissue compartments (e.g., inside and outside a blood vessel). A smaller beam waist and a smaller DOF lead to better image resolution in the xy and z directions, clearer structures that can be observed, and a smaller point spread function. At the DOF, the focal spot area is blurred to twice of that at the beam waist w_0.

The intensity of a G beam in 2PF (I_{2p}) is proportional to the square of the intensity I_G, i.e.,

$$I_{2P} \propto \eta\sigma_2 {I_G}^2(r,z), \tag{9}$$

where η is the fluorescence efficiency, and σ_2 is the two-photon dye cross section with the unit GM and $1\ \mathrm{GM} = 10^{-50}\ \mathrm{cm}^4\,\mathrm{s/photon}$.[3] The intensity I_{2p} is used to locate the excitation value of 2PF. It spreads over $2z_0$ at the z axis, reduces to $1/4I_0$ at z_0 [Fig. 2(b)], and falls off fast to $e^{-4}I_0$ at the beam waist ($r = w_0$ and $z = 0$).

The size of the 2PF image pattern follows ${I_G}^2$ in the xz plane. Figure 3(a) illustrates the schematic of a microvessel with diameter d in brain tissue, where $d > 2z_0$ and $d > 2w_0$, and the x axis is along the vessel axial direction. The size of the 2PF oval in the yz plane [Fig. 3(b)] is the spatial convolution of the G beam and the emitting particle of diameter d. Since the indices of tissue refraction and solvent are close, the reflection coefficient with index $n = 1.375$ at the boundaries[4] matches the little change in intensity due to the reflection of the vessel wall.

Figure 4(a) shows the convolution of a G beam and the emission of a particle at size d, where $d < 2z_0$ and $d < 2w_0$. The 2PF image pattern is an ellipse with the major axis $2z_0$ (DOF)[5] and the minor axis $2w_0$. Figure 4(b) from Chaigneau et al.[6] shows an example of a 2PF image of green beads (200 nm) on brain tissue layer; the image was distorted since the size of the particle was smaller than $2w_0$ and $2z_0$, and corrections for the wavefront distortion were made.

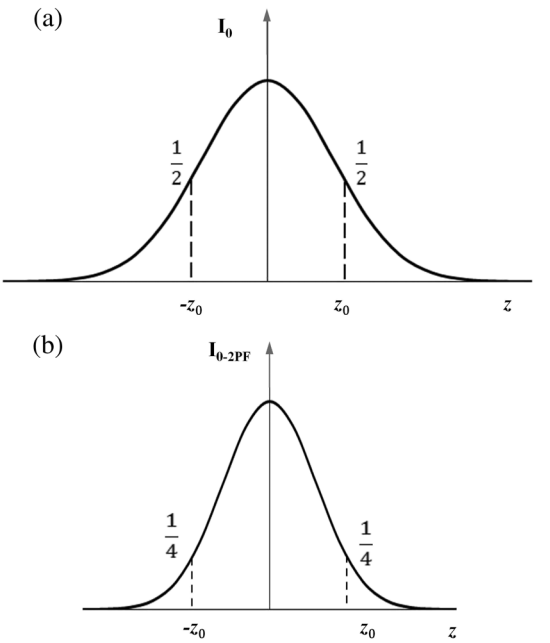

Fig. 2 Axial intensity of a Gaussian beam as a function of z at $r = 0$. (a) At $z = 0$, intensity decreases to 1/2 at z_0. (b) Two-photon fluorescent (2PF) intensity profile in which the intensity decreases to 1/4 at z_0.

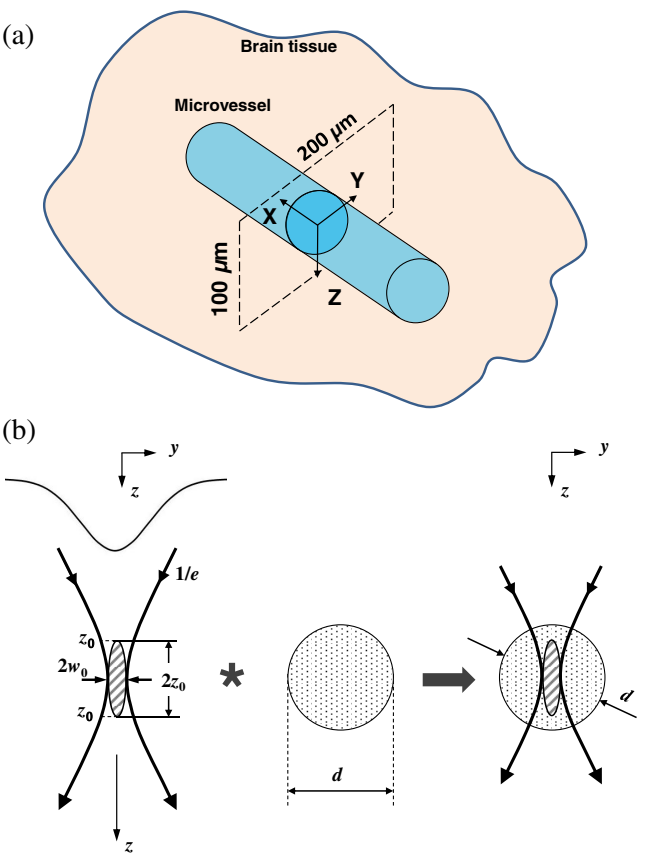

Fig. 3 (a) Schematic of a microvessel in the brain. The z direction is the laser beam scanning direction. (b) Convolution of a Gaussian beam profile with a vessel of diameter d ($d > 2w_0$ and $d > 2z_0$) yields the 2PF pattern of scanning in yz plane.

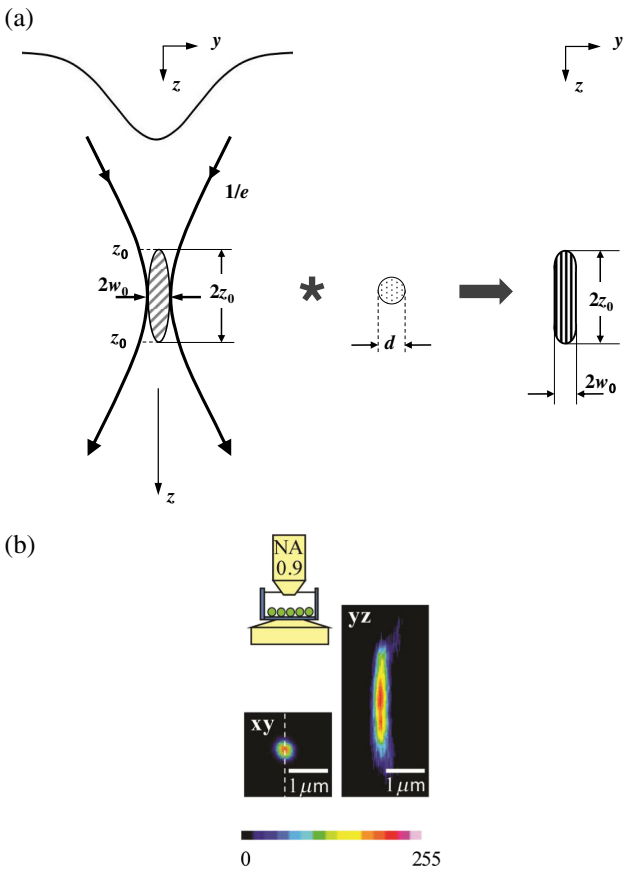

Fig. 4 (a) Convolution of a Gaussian beam profile with a vessel of diameter d ($d < 2w_0$ and $d < 2z_0$) yields the 2PF pattern of scanning in yz plane. (b) Image of 2PF of emitter particle (beads, $d = 200$ nm $< 2z_0$) [adapted from Fig. 2(a), Ref. 6].

2.2 *Animal Preparation*

Adult female Sprague–Dawley rats (250 to 300 g, age 3 to 4 months, Hilltop Laboratory Animals Inc., Scottdale, Pennsylvania) were used for in vivo experiments. All procedures and the animals use were approved by the Institutional Animal Care and Use Committee of the City College of New York. The detailed procedure was similar to that described in Ref. 7. Briefly, the rat was subcutaneously anesthetized with pentobarbital sodium, and then its skull was exposed by shaving off the hair and cutting away the skin and connective tissue. The frontoparietal bone (left or right) was carefully thinned with a high speed microgrinder (0 to 50,000 rpm, DLT 50KBU, Brasseler, GA) until a portion of it (~4 × 6 mm) became soft and translucent. After skull grinding, the left (or right) carotid artery was cannulated with a PE50 tubing. The rat was then put on a stereotaxic instrument (David Kopf Instruments) with its head fixed with two ear bars and a mouth clamp.

Cerebral microvessels (diameter 20 to 40 μm) were observed with a two-photon microscope (40×, NA = 0.8, water immersion, Olympus) through the thinned part of the skull. FITC-dextran-70k (FD70s, Sigma; MW 70,000, Stokes radius ~3.6 nm; emits at 520 nm) solution, concentration 1 mg/ml in 1% bovine serum albumin Ringer, was then injected into the cerebral circulation via the tubing at a perfusion rate of 3 ml/ min.

2.3 *Two-Photon Microscopy and Image Collection*

An Ultima two-photon microscope (Prairie Tech. Inc., WI, excitation wavelengths 680 to 1080 nm) was used in the experiments. FITC-dextran-70k solute was excited with 140-fs laser pulses at 800 nm using Ti-Sapphire laser (Chameleon Ultra II laser, Coherent Inc.), and the fluorescence emitted from the brain specimen was collected by the photomultiplier tubes after passing the barrier filter (525 ± 35 nm). For this imaging system w_0 is ~0.5 μm, z_0 is ~1 μm, and the DOF is ~2 μm.

When the fluorescence solution was injected into the cerebral circulation, images were simultaneously recorded. The images were collected as image stacks in the z direction every 5 s, and were reconstructed into a segment with the cross-sectional area of 200 × 100 μm (y-z) and thickness of 8 μm [Fig. 3(a)]. Collected images were analyzed offline for measuring the light intensity profile inside and outside the microvessel.

3 Results and Discussions

Figure 5 demonstrates the cross-sectional light intensity profile of a cerebral microvessel filled with fluorescein dye (FITC-dextran-70 k) in rat brain tissue. The light intensity profiles (I), at different cross-sectional distances from the center of the lumen were digitized to show variations on the 2P emission of fluorescein dye in the y and z directions, respectively. Comparison of the intensity plots for track lines 1, 2, and 3 demonstrated that the closer the cross section is to the center of the lumen, the higher the peak intensity and the wider the spectral peak width are. Since the diameter of the cerebral microvessel imaged (20 to 40 μm) was much larger than $2w_0$ and $2z_0$, there was no distortion in the images and no correction was needed for vessel structure reconstruction. In addition, the light intensity profile can be used for the determination of microvessel permeability and solute diffusion coefficient in the brain tissue,[7] since the fluorescein dye travels from the vessel lumen to the brain tissue passing through the vessel wall.

An important feature of the 2PF imaging of G beam is that its emission occurs in regions that are occupied by G beam as the beam scans. The G beam scans first in the xy plane and then along the z direction. The resulting 2PF intensity is plotted in the xy plane at $z = 0$, and the intensity of the G beam $I_G{}^2$ is plotted in the yz (or xz) plane. The length of the yz plot is $2z_0$ and the diameter of the vessel or particle is d. A small $2z_0$ is needed to obtain the actual images of a vessel in the z direction without any image correction, which is typically 2 μm when using a 40× lens.

Another important feature in 2PF imaging is the excitation wavelength. To attain the deepest penetration, due to linear absorption of the host media the wavelength should be within the range of 700 to 900 nm, typically around 800 nm. The image is blurred by multiscattering in the tissue where the limit of coherent penetration of the ballistic pulse intensity is governed by scattering length (Ls). The transport scattering length (Ltr) governs the distance to change the photon direction (typically 5 to 8 Ls). Typical Ltr used in optical coherence tomography is about 0.5 to 1 mm for tissues where the diffusion equation becomes valid for 8× Ltr scattering length.[8,9] The effect of multiscattering in a Gaussian profile is discussed in detail by Ying et al.[5] The Ls for brain tissue is about 80 μm and the Ltr is approximately 480 μm. The imaging depth of 500 μm in brain tissue can be achieved in theory.

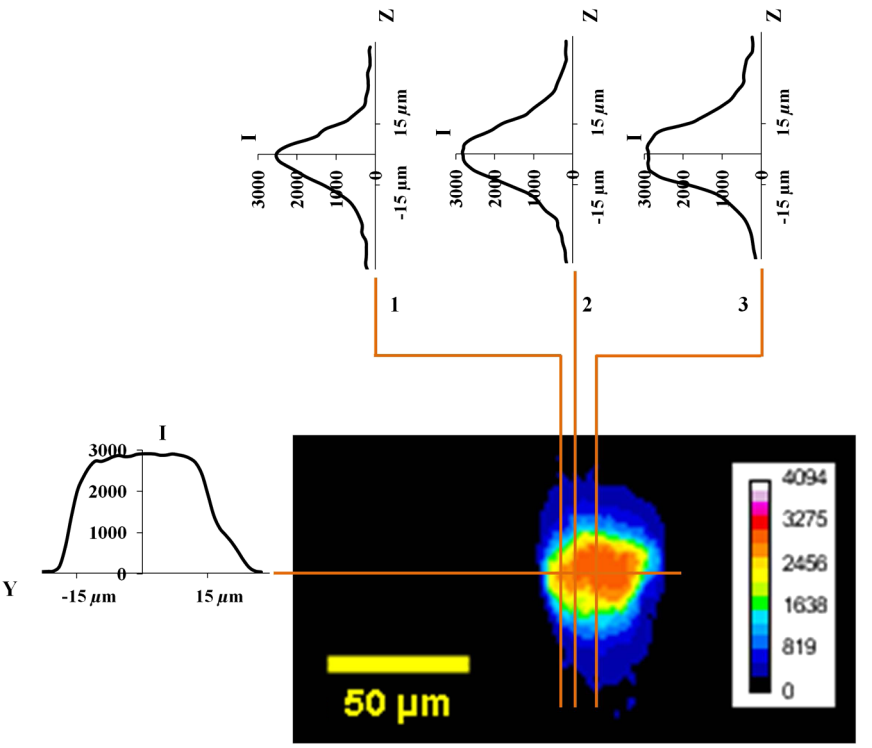

Fig. 5 Distribution of 2PF intensity profiles in the cross-sectional view of a rat brain microvessel in *y* and *z* directions. Different spatial positions were digitized at vertical direction of the vessel lumen. Track line 1, the cross section at 1/4 radius; track line 2, the cross section at 1/2 radius; track line 3, the cross section in the middle. The size of vessel diameter $d > 2w_0$ and $2z_0$ gives full resolution.

The spatial resolution may be improved when the G beam has a smaller beam waist w_0 or Rayleigh length z_0, which introduces the application of 3PF or four-photon fluorescence (4PF). For example, by substituting Eq. (2) into Eq. (1) and applying Eq. (9), the intensity of 2PF is given as

$$I_{2P} \propto \eta\sigma_2 {I_G}^2 = \eta\sigma_2 \left[\frac{I_0}{1+(z/z_0)^2}\right]^2 \exp\left[-\frac{4r^2}{w^2(z)}\right]. \quad (10)$$

The beam intensity falls off to approximately $\propto 1/z^4$ when $z \gg z_0$. The beam waist of the 2P intensity profile is

$$w_0^{2P} = \frac{1}{\sqrt{2}} w_0. \quad (11)$$

For 3PF, the intensity (I_{3P}) is obtained similarly as

$$I_{3P} \propto \eta\sigma_3 {I_G}^3 = \sigma_3 \left[\frac{I_0}{1+(z/z_0)^2}\right]^3 \exp\left[-\frac{6r^2}{w^2(z)}\right], \quad (12)$$

where σ_3 is the particle 3P cross section with dye with the unit of 10^{-80} cm^6 s^2/photon^2.[10] The beam intensity falls off to approximately $\propto \sim 1/z^6$ when $z \gg z_0$. The beam waist of 3P intensity profile is

$$w_0^{3P} = \frac{1}{\sqrt{3}} w_0. \quad (13)$$

Similarly, for 4PF, the intensity (I_{4P}) is

$$I_{4P} \propto \eta\sigma_4 {I_G}^4 = \sigma_4 \left[\frac{I_0}{1+(z/z_0)^2}\right]^4 \exp\left[-\frac{8r^2}{w^2(z)}\right], \quad (14)$$

where σ_4 is the particle 4P cross section with dye with the unit of 10^{-109} cm^8 s^3/photon^3.[10] The beam intensity falls off to approximately $\propto \sim 1/z^8$ when $z \gg z_0$. The beam waist of 4P intensity profile is

$$w_0^{4P} = \frac{1}{2} w_0. \quad (15)$$

The salient parameters of 2P, 3P, and 4P imaging are compared in Table 1. The reduction of the beam waist w_0 from 2PF to 4PF will lead to higher spatial resolutions in the *x*-*y* plane. Equation (3) shows that a longer wavelength λ will lead to a

Table 1 Spatial parameters for multiphoton fluorescence.

Beam type	1P	2P	3P	4P
Beam waist	w_0	$w_0/\sqrt{2}$	$w_0/\sqrt{3}$	$w_0/2$
Fall off distance	$\propto (1/z^2)$	$\propto (1/z^4)$	$\propto (1/z^6)$	$\propto (1/z^8)$
DOF	$2z_0$	$1.28z_0$	z_0	$0.82z_0$
Intensity at beam waist	e^{-2}	e^{-4}	e^{-6}	e^{-8}

shorter Rayleigh length z_0; therefore, an increase of the wavelength from 2PF to 4PF will result in higher spatial resolution in the z axis. Using 3PF or 4PF other than 2PF shows a promising way to improve imaging resolution; however, *in vitro* or *in vivo* experiments are still needed to further investigate the improvement both qualitatively and quantitatively.

A Gaussian beam is superior to a Bessel beam for backward and forward multiphoton microscopes with applications in 3-D imaging. Since the focal spot of the Gaussian beam is well localized compared to the long line of a Bessel beam, Gaussian beam is commonly used for optical slicing and 3-D reconstruction. The Bessel beam is diffraction free and well collimated over long distances (>1 mm) with surrounding rings. It works well in multiphoton arrangement excitation in perpendicular viewing and scanning, and can be used in light sheet microscopy to generate 2-D and to some extent 3-D images of thick media.[11–13] However, in the multiphoton excitation process, only approximately 5% of the Bessel beam is in the central spot while a large amount is lost in the rings, and since these rings are not important in the formation of images, the long collimated Bessel beam may not be used to locate nanometer-scale structures in the z-axis. Thus, a Gaussian beam overcomes this disadvantage of the Bessel beam, and is used to locate nanometer structures in z-stacks acquired with the backward transmission microscope.

In conclusion, this study examines the critical properties of a Gaussian beam for biologists and biomedical engineers who are using 2P or multiphoton microscope. The spatial forms of Gaussian beam (w_0 and z_0), with micrometer-scale resolution, provide the information needed for determining microvessel permeability and solute diffusion coefficients in tissue. With the application of 2P or multiphoton microscopy, high resolution imaging of tissue or vessels can be obtained. This work can be used to investigate neuronal or vascular structure in physiological or biological process *in vivo* or *ex vivo*.

Acknowledgments

We thank Dr. Bingmei M. Fu for providing rats. This work was partially supported by ARO research grants, and by NIH (Grant Nos. G12-RR003060 (NCRR/RCMI) and SC1HD068129).

References

1. B. E. A. Saleh and M. C. Teich, "Beam optics," in *Proc. Fundamentals of Photonics*, pp. 80–107, John Wiley & Sons, New York (1991).
2. A. Yariv, *Quantum Electronics*, 3rd ed., Wiley, New York (1989).
3. M. Drobizhev et al., "Two-photon absorption properties of fluorescent proteins," *Nat. Methods* **8**(5), 393–399 (2011).
4. T. Lister, P. A. Wright, and P. H. Chappell, "Optical properties of human skin," *J. Biomed. Opt.* **17**(9), 090901 (2012).
5. J. P. Ying, F. Liu, and R. R. Alfano, "Spatial distribution of two-photon-excited fluorescence in scattering media," *Appl. Opt.* **38**(10), 2151–2151 (1999).
6. E. Chaigneau et al., "Impact of wavefront distortion and scattering on two-photon microscopy in mammalian brain tissue," *Opt. Express* **19**(23), 22755–22774 (2011).
7. L. Shi et al., "Quantification of blood-brain barrier solute permeability and brain transport by multiphoton microscopy," *J. Biomech. Eng.* **136**(3), 031005 (2014).
8. A. Yaroshevsky et al., "Transition from the ballistic to the diffusive regime in a turbid medium," *Opt. Lett.* **36**(8), 1395–1397 (2011).
9. K. M. Yoo, F. Liu, and R. R. Alfano, "When does the diffusion-approximation fail to describe photon transport in random-media," *Phys. Rev. Lett.* **64**(22), 2647–2650 (1990).
10. D. S. Corrêa et al., "Z-scan theoretical analysis for three-, four- and five-photon absorptions," *Opt. Commun.* **277**(2), 440–445 (2007).
11. F. O. Fahrbach et al., "Light-sheet microscopy in thick media using scanned Bessel beams and two-photon fluorescence excitation," *Opt. Express* **21**(11), 13824–13839 (2013).
12. Y. Lin et al., "Experimental investigation of Bessel beam characteristics," *Appl. Opt.* **31**(15), 2708–2713 (1992).
13. J. Durnin, J. J. Miceli, Jr., and J. H. Eberly, "Comparison of Bessel and Gaussian beams," *Opt. Lett.* **13**(2), 79–80 (1988).

Lingyan Shi is a research associate at IUSL and Biology Department at the City College of New York (CCNY). She obtained her PhD degree in biomedical engineering from CCNY. Her research interests include *in vivo* deep tissue imaging by using multiphoton with femtosecond laser pulses to understand functional interactions between neural cells and brain vasculature, and quantification/regulation of blood–brain barrier permeability for drug delivery. Other research interests include biomedical optics and cardiovascular biomechanics.

Adrián Rodríguez-Contreras is a biology assistant professor at the City College of New York. In 2008, he established the developmental neurobiology laboratory combining anatomical, electrophysiological, and two-photon microscopy tools to study brain development in rodents and barn owls. Other research interests include applying novel methods in fluorescence microscopy for *in vivo* studies, exploring the cellular mechanisms involved in the growth of brain tumors and understanding the functional interactions between neural cells and the brain vasculature.

Robert R. Alfano is a distinguished professor of science and engineering at the City College of CUNY. He has pioneered many applications of light and photonics technologies to the study of biological, biomedical, and condensed matter systems, invented and used in his research supercontinuum and novel tunable solid-state lasers. He has received his PhD in physics from New York University and is a fellow of the American Physical Society, Optical Society of America, and IEEE.